

## Flexible and Printed Electronics



### PAPER

# Synthesis and characterization of PEDOT-PEGDA blends for bioelectronic applications: surface properties and effects on cell morphology

RECEIVED  
23 July 2019

REVISED  
20 December 2019

ACCEPTED FOR PUBLICATION  
30 January 2020

PUBLISHED  
26 February 2020

Giuseppina Polino<sup>1,2,6,7</sup> , Claudia Lubrano<sup>1,3,7</sup>, Paola Scognamiglio<sup>1</sup>, Valentina Mollo<sup>1</sup>, Selene De Martino<sup>1</sup>, Giuseppe Ciccone<sup>1,5,8</sup>, Laura Matino<sup>1,3</sup>, Angela Langella<sup>1,4</sup>, Paolo Netti<sup>1,3,4</sup>, Aldo Di Carlo<sup>2</sup> , Francesca Brunetti<sup>2</sup> and Francesca Santoro<sup>1</sup> 

<sup>1</sup> Center for Advanced Biomaterials for Healthcare, Istituto Italiano di Tecnologia, I-80125 Napoli, Italy

<sup>2</sup> Center for Hybrid and Organic Solar Energy (CHOSE) Department of Electronic Engineering, University of Rome Tor Vergata, Via del Politecnico 1, I-00133 Rome, Italy

<sup>3</sup> Dipartimento di Chimica, Materiali e Produzione Industriale (DICMAPI), Università di Napoli Federico II, P.le Tecchio 80, Napoli, Italy

<sup>4</sup> Centro di Ricerca Interdipartimentale sui Biomateriali (CRIB), Università di Napoli Federico II, P.le Tecchio 80, Napoli, Italy

<sup>5</sup> Dresden Integrated Center for Applied Physics and Photonic Materials (IAPP), Institute for Applied Physics, Technische Universität Dresden, Dresden, Germany

<sup>6</sup> Current affiliation: Center for Hybrid and Organic Solar Energy (CHOSE) Department of Electronic Engineering, University of Rome Tor Vergata, Via del Politecnico 1, I-00133 Rome, Italy

<sup>7</sup> These authors have contributed equally.

<sup>8</sup> Current affiliation: Dresden Integrated Center for Applied Physics and Photonic Materials (IAPP), Institute for Applied Physics, Technische Universität Dresden, Dresden, Germany.

E-mail: [giuseppina.polino@uniroma2.it](mailto:giuseppina.polino@uniroma2.it)

**Keywords:** Poly(3, 4-ethylenedioxythiophenes) blends, conductive films, tissue engineering, spin coating, spray coating

Supplementary material for this article is available [online](#)

### Abstract

One of the burning questions in bioelectronics concerns the discovery of new materials which might properly couple the conductive properties of historical metallic electrodes and the softness of hydrogels structures, widely employed for engineered cell culture. This demand leads to the massive increase in the use of conductive polymers (CPs), such as Poly(3, 4-ethylenedioxythiophenes) (PEDOT:PSS) mixed with other polymers in order to reach the best compromise among conductivity, surface morphology and biocompatibility. In this work, we tested multiple blends of (PEDOT:PSS) with different percentages of poly(ethylene glycol) diacrylate (PEGDA), a photoactive crosslinker which is highly employed for fabricating biomimetic interfaces. We carried out an accurate electrical and topographical characterization, also comparing spin and spray deposition techniques. The resulting blends were tested as cell culture substrates for primary fibroblasts cells. The biocompatibility and morphological analysis revealed that these materials can be suitable for this cell line. The best results in terms of conductivity, morphology and biocompatibility was accomplished in the case of the mixture PEDOT:PSS 8% PEGDA, which provides an essential starting point for future development of 3D organic electrodes and bioelectronics interfaces to be coupled with biological systems.

Conducting polymers (CPs) are widely used as interfaces between electronics and biology due to their mechanical and chemical properties, which are compatible with the composition of biological tissues and cells [1]. The strength of the conjugated polymers is represented by their appreciable conductivity and their chemical nature, which grants the possibility to engineer these materials in various forms, exerting a Young's modulus which well fits those of biological

tissues. These materials can be integrated with a plethora of mechanical supports, giving the possibility to realize conformable, stretchable, fibrous and 3D interfaces for integration with biological systems. For these reasons, CPs offer a great variety of applications, such as neural electrodes or organic transistors, allowing the contact with aqueous solutions with a high salt concentration, which are corrosive to traditional electronic materials [2]. Among several

applications, conjugated polymers can support and eventually facilitate the *in vitro* adhesion, proliferation and differentiation of various cell types [3]. When used for cell culture purposes, CPs might be blended with other polymers (i.e. PLA, PLGA, PCL) in order to vary, for instance, the surface morphology as well as the mechanical properties. In this way, the resulting material can be integrated in more complex devices providing an optimal interface for cells, recapitulating the extracellular matrix environment as well as exploiting sensing/stimulating processes at the interface through application of electrical fields. Furthermore, the contact area with cells might be further improved by chemical functionalization with biomolecules [4] such as DNA [5], peptides [6], lipid bilayers [7], growth factors [8], components from the extracellular matrix [9, 10].

Among various conjugated polymers engineered in the last decades, PEDOT:PSS is highly conductive and has found major applications in bioelectronics and tissue engineering for its environmental stability and processability [11, 12]. In fact, it can be processed in the form of thin films by spin-coating or large area deposition methods such as spray-coating [13, 14] as well as in 3D architectures like scaffolds [15]. In the last years, PEDOT:PSS has been also processed with bio-dopants and as composite [16] to modulate its suitability for the bioelectronic coupling with cells [17]. Furthermore, PEDOT:PSS-based materials have been recently modified with polymers commonly used in tissue engineering, such as polyethylene glycol (PEG) and its diacrylated forms (PEGDA). In fact, it has been widely used for fabrication of biomimetic substrates with tunable features (i.e. swelling [18]) and patternability [19] thanks to the photosensitive properties of the acrylate chains [20]. Moreover, PEDOT:PSS-PEGDA composites have shown the potential of offering a biomimetic environment with tunable geometrical properties through lithographic processes [21]. Therefore, depending on the application (i.e. cell culture, biosensing, biomodulation), the electroactive properties could be finely tuned to match the appropriate requirements, spanning at different scales. A key role among the properties of the PEGDA-based scaffolds for tissue engineering is given to the swelling ratio. In the recent years, conductive hydrogels scaffolds have been proposed [22, 23] to induce both mechanical and electrical stimuli to the cells [24, 25]. Therefore, for this kind of application, the swelling ratio must be maximized, and its role is crucial since it guarantees the essential and dynamic mechanical loading that the biological cells need. However, the synthesis of PEDOT:PSS-PEGDA platforms might include multiple-step polymerization and, in many cases, the resulting blend maybe not as conductive to provide enough charge transfer for efficient cell stimulation or probing.

Here, we developed different electrodes based on PEDOT:PSS-PEGDA which were deposited in a one-step procedure by spin or spray coating. Moreover, in this work, conductive polymeric films are investigated as possible materials for bioelectronic purposes, and

the swelling behavior of PEDOT:PSS interfaced with electrolyte is therefore evaluated. However, with a view on using these materials as electrodes for interfacing optoelectronic devices with living systems, the PEDOT:PSS based films must require the minimization of the swelling ratio, in order to limit water uptake and catastrophic failure of such devices [26]. The conductivity of the electrodes has been increased by adding ethylene glycol (EG). The films were characterized morphologically (scanning electron microscopy- SEM and atom force microscopy-AFM) and the conductivity was investigated via electrochemical impedance spectroscopy (EIS).

Finally, viability studies were performed to address the biocompatibility of the films, and the cellular adhesion/spreading. Finally, we resolved the interface between the cellular membrane and the surface of the spin and spray-coated solutions.

## Materials and methods

### Preparation of PEDOT:PSS films

PEDOT:PSS films were deposited using the pristine solution (Clevios PH1000, Heraeus), modifying the basic composition with 6% wt ethylene glycol (EG, Sigma Aldrich) and different percentages of polyethylene glycol diacrylate (PEG from 2% to 17% wt, Sigma Aldrich). The solutions were diluted 1:2 v/v in ethanol (Sigma Aldrich) and stirred at room temperature overnight prior to use. Glass microslides (25 mm × 25 mm) were cleaned in an ultrasonic bath at 40 °C in deionized water, followed by non-ionic detergent (PF7), deionized water, acetone (Sigma Aldrich) and ethanol (Sigma Aldrich). Each step had a duration of 10 min until a final drying under a nitrogen flow was performed. PEDOT:PSS-based films were deposited by spin and spray-coating techniques. Spin-coating was carried out at 800 rpm (acceleration 1000 rpm s<sup>-1</sup>) for 60 s (~100 ± 30 nm). Spray-coating was performed on a hot plate with a temperature of 120 °C by using a dual-action commercial airbrush supplied by compressed air. To control the thickness of the film, PEDOT:PSS solutions were sprayed for 60 s with a pressure of 1 bar and a nozzle to sample distance of 15 cm (film thickness ~150 ± 60 nm). After both spin-coating and spray-coating, the films were dried at 150 °C for 30 min to remove residual solvents. In order to evaluate the swelling behavior of the film, the blends at different concentration of PEGDA are weighed (wet) and crosslinked under UV lamp (Dymax EC 5000 UV lamp) (power density of 225 mW cm<sup>-2</sup>). The samples were left to soak on phosphate buffer saline (PBS) (Sigma Aldrich) after UV-crosslinking. The wet samples were weighted after 10, 20, 90 and 180 min of soaking, removing the excess PBS from the surface of the material. The substrates were then dried in oven overnight at 60 °C, to obtain the dry weight.

### Electrochemical film characterization

EIS was performed at room temperature using a potentiostat (PGSTAT302N, Metrohm Autolab B.V.). To evaluate the electrochemical properties of the deposited films, we used PBS as electrolyte solution. The sinusoidal input signal was set to 10 mV by scanning a range of frequencies from 1 Hz to 100 kHz. We used a two-electrodes configuration and a platinum (Pt) electrode was used as reference electrode and immersed in the electrolyte during the measurements.

### Atomic force microscopy (AFM)

We used a JPK NanoWizard II (JPK Instruments), mounted on the stage of an Axio Observer Z1 microscope (Zeiss) to characterize the PEDOT:PSS films. Commercial silicon nitride tips (MLCT, Bruker) with a resonance frequency of 50 kHz and a spring constant of  $0.10 \text{ N m}^{-1}$  were used to scan in the contact mode in air all over the sample area of interest.

### Sample sterilization and functionalization

Samples were washed 2 times in distilled water, sterilized in 70% ethanol for 2 min and a final wash was performed with distilled water. PEDOT:PSS based films were functionalized with poly-L-lysine (PLL, Sigma Aldrich). 0.01% PLL (aqueous solution) was incubated on the films at 37 °C overnight. Samples were washed with distilled water shortly before cells' plating.

### Cell culture

The primary cells were collected through dissection from chicken embryos (12 d old) tissues fibroblasts [27]. In particular with the help of a scissor, the back tissue was collected, fragmented and then incubated in a solution of Trypsin-EDTA 2.5% (Life Technologies), PBS with Calcium and Magnesium (Sigma Aldrich) and Collagenase II (Sigma Aldrich,  $100 \text{ U ml}^{-1}$ ) for 5 min at 37 °C. The supernatant was then transferred into a new tube with fresh medium to quench the action of trypsin and centrifugate for 10 min at 1000 rpm. After removing the supernatant, the pellet was resuspended in 3 ml of fresh medium and plated into a 25 mm<sup>2</sup> flask. Cells were cultured in DMEM: Ham-F12 (1:1) media (Sigma Aldrich) supplemented with 10% fetal bovine serum (Sigma-Aldrich), 1% penicillin/streptomycin (Sigma Aldrich), 1% L-Glutamine (Sigma-Aldrich), and ascorbic acid (Sigma Aldrich)  $100 \mu\text{M}$  in a 5% CO<sub>2</sub> incubator at 37 °C.

Confluent fibroblasts were trypsinated and seeded on planar PEDOT:PSS substrates at a density of  $100\,000 \text{ cells cm}^{-2}$  and left in the incubator at 37 °C.

### Biocompatibility assay

After 1 d *in vitro* (DIV), primary fibroblasts were labeled with a solution of Calcein-AM (Sigma Aldrich, final concentration  $1 \mu\text{g ml}^{-1}$ ) and Propidium Iodide (Thermo Fisher, final concentration  $10 \mu\text{g ml}^{-1}$ ) in

PBS and incubated at 37 °C for 10 min. Finally, the samples were washed with PBS before imaging.

### Cells morphology analysis

Cells morphology was analyzed through actin staining with Phalloidin-555 (Abcam), while nuclei were stained with Draq5 (Abcam). For the staining procedure, cells were fixed in 4% paraformaldehyde (Società Italiana Chimici) for 15 min at room temperature and then washed 3 times with PBS. The cell membrane was permeabilized through incubation with 0.1% Triton-X (Sigma Aldrich) in PBS for 5 min at room temperature, followed by incubation for 30 min at room temperature with Phalloidin-555 (diluted 1:1000 in PBS). Finally, the nuclei staining was performed through incubation with Draq5 (diluted 1:1000 in PBS) for 15 min.

### Thin resin plasticization of cells

Samples with cells were prepared using a thin plasticization protocol as previously presented [28, 29]. In brief, cells were fixed in 2.5% glutaraldehyde (Electron Microscopy Sciences) in  $0.1 \text{ mol l}^{-1}$  sodium cacodylate buffer (pH 7.3, Electron Microscopy Sciences) at 4 °C overnight, washed 3 times in the same buffer and quenched in 20 mM glycine (Sigma Aldrich) for 20 min at 4 °C. After rinsing with buffer ( $3 \times 5 \text{ min}$  at 4 °C), specimens were post-fixed with equal volumes of 4% osmium tetroxide (Electron Microscopy Sciences) and 2% potassium ferrocyanide (Electron Microscopy Sciences) for 1 h on ice, then washed ( $3 \times 5 \text{ min}$ ) with chilled buffer. Samples were incubated with 1% thiocarbohydrazide (Electron Microscopy Sciences) at room temperature for 20 min and washed ( $3 \times 5 \text{ min}$ ) in distilled water. The thiocarbohydrazide solution was freshly prepared by adding the solid compounds to distilled water at 60 °C with intermittent shaking for at least 1 h followed by cooling at room temperature. Substrates with cells were post fixed with 2% osmium tetroxide (aqueous solution) for 1 h at room temperature, washed 3 times in distilled water and *en-bloc* stained with 4% aqueous uranyl acetate (Sigma Aldrich) overnight at 4 °C. After rinsing with chilled deionized water, specimens were treated in 0.15% tannic acid buffer for 3 min and again rinsed ( $3 \times 5 \text{ min}$ ) with water. The cells were dehydrated in increasing concentration of ethanol (10%, 30%, 50%, 70%, 90%, 100%, Sigma-Aldrich)). Each step was performed for 10 min on ice, except for the last step in 100% ethanol solution that was performed at room temperature. Substrate with cells were infiltrated with increasing concentration of Spurr's low viscosity embedding resin (Electron Microscopy Sciences) in absolute ethanol, at room temperature in a sealed container, using these ratios: 1:3 ( $2 \times 3 \text{ h}$ ), 1:2 ( $2 \times 3 \text{ h}$ ), 1:1 (overnight), 1:2 ( $2 \times 3 \text{ h}$ ), 2:1 ( $2 \times 3 \text{ h}$ ), 3:1 ( $2 \times 3 \text{ h}$ ). Spurr-ethanol mixture was replaced with freshly 100% Spurr's resin and samples were infiltrated at room temperature overnight. To

remove the excess of resin, each specimen was mounted vertically for 2 h, and then quickly rinsed with absolute ethanol prior to polymerization in oven at 70 °C overnight. Samples were glued with colloidal silver paste (Ted Pella Inc.) to a pin stub and a 10 nm layer of platinum–palladium alloy was deposited by using a HR 208 Sputter Coater (Cressington) before imaging.

### Fluorescence imaging and analysis

Optical observations were carried out with an Axiobserver-Z1 (Zeiss) using a 10× (for biocompatibility experiment) and 40× (for cell morphology analysis). Images were acquired with a Colibrì 2 LED lamp emitting light at 4 different wavelengths: 365, 470, 555 and 625 nm. The emission bands were selected by specific interference filters. In particular we employed the following wavelengths: Calcein AM  $\lambda_{\text{ex}} = 470$  nm and  $\lambda_{\text{em}} = 500$ –530 nm, propidium iodide  $\lambda_{\text{ex}} = 555$  nm  $\lambda_{\text{em}} = 580$ –630 nm; Nuclei (Draq5)  $\lambda_{\text{ex}} = 625$  nm  $\lambda_{\text{em}} = 640$ –710 nm, actin cytoskeleton (Phalloidin)  $\lambda_{\text{ex}} = 555$  nm  $\lambda_{\text{em}} = 570$ –610 nm. 3 experiments were carried out and  $N = 3$  samples per type were analyzed. 5 frames per sample type were acquired, processed and analyzed with the software ImageJ (NIH). Particularly, the biocompatibility was evaluated by identifying two cell populations: live and dead cells, and after counting we made a statistical analysis by normalizing each cells' population to the total number of cells.

A threshold in the fluorescence images was set for the cells morphology analysis, and then the watershed function allowed to locate a region of interest (ROI) corresponding to single cells area. Once located the ROI, the program will automatically fit each section into an ellipse and calculate the major and minor axis, the area and the perimeter in order to extrapolate the shapes descriptors roundness ( $\theta$ ) and circularity ( $\chi$ ).

The statistical analysis was performed with Origin software.

### SEM imaging and FIB sectioning

Scanning electron microscopy imaging was performed with 5–15 kV beam acceleration voltage, with a 30 micrometers aperture to detect secondary electrons and backscattered electrons with a pixel resolution of  $1024 \times 1024$ . For the sectioning, a dual-beam machine (Helios Nanolab 350, ThermoFisher) was used, and the procedure was adapted from the work of Santoro *et al* [29].

## Results and discussion

Conductive polymers blends have been obtained by mixing PEDOT:PSS with ethylene glycol (EG), which is able to increase conductivity [30], and different amounts of PEGDA.

The films were then deposited by spin and spray-coating as described in the figure 1 in which is shown exemplary scanning electron and atomic force

micrographs of spin and spray-coated films realized with Pristine PEDOT:PSS (A), 2% PEGDA (B) and 8% PEGDA (C). As expected, the addition of the PEGDA polymer induces a higher roughness at the surface as similarly observed for PEDOT:PSS-PEGDA blends obtained with a two-step polymerization process [21]. supplementary information S1(A), (B) is available online at [stacks.iop.org/FPE/5/014012/mmedia](https://stacks.iop.org/FPE/5/014012/mmedia) shows the morphological characterization of PEDOT:PSS + EG and films modified with 17% PEGDA. PEDOT:PSS + EG films have in general a smooth surface both in the cases of spin and spray-coating. When PEGDA is added, a local roughness in the range of 300–580 nm is determined for the films which are deposited via spray-coating (figures 1(B), (C)). This might be induced by the increased viscosity of the solution [31]. In addition, typical topographies are introduced by spray-coating because of the bulk liquid that transforms into small droplets [32]. Moreover, when the film is deposited and the solvent evaporates, island-like typical of the Marangoni's flows can be detected [33]. Spheroidal structures can be depicted on PEDOT:PSS:PSS films when a low concentration (2%) of PEGDA dopant is used for both spin and spray-coating procedures (figure 1(B)). We can observe that the dopant amount changes the morphology of PEDOT:PSS film inducing a non-homogeneous structure with higher interface area. The SEM characterization confirms that the poor solubility of low-concentrated PEGDA in PEDOT:PSS mixtures induces defects in the film deposition as also reported in the work of Caironi *et al* [34].

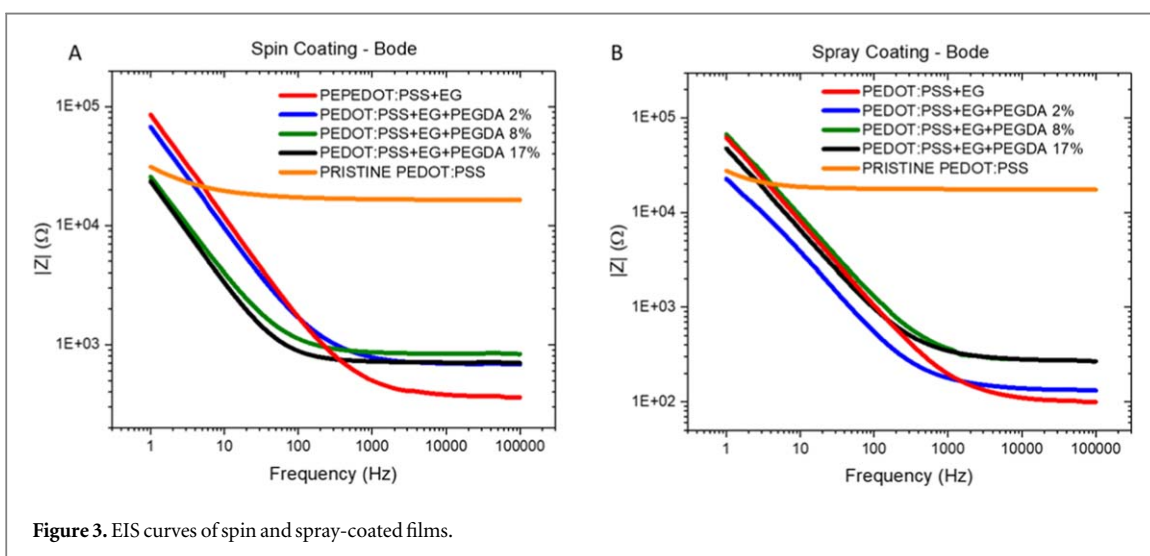
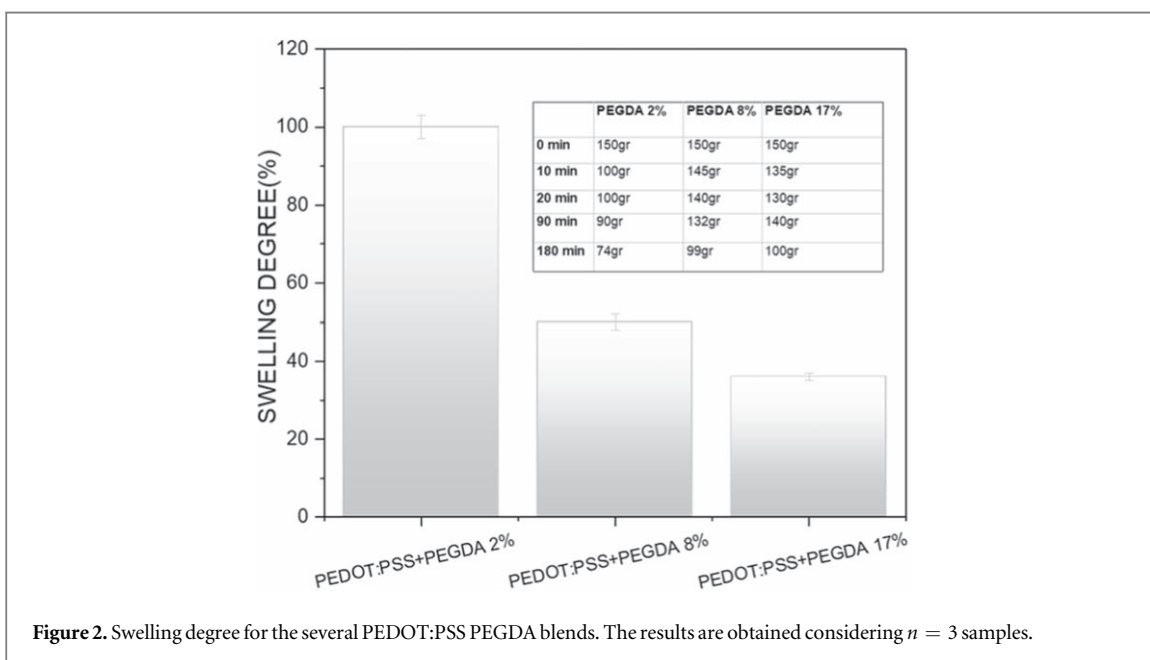
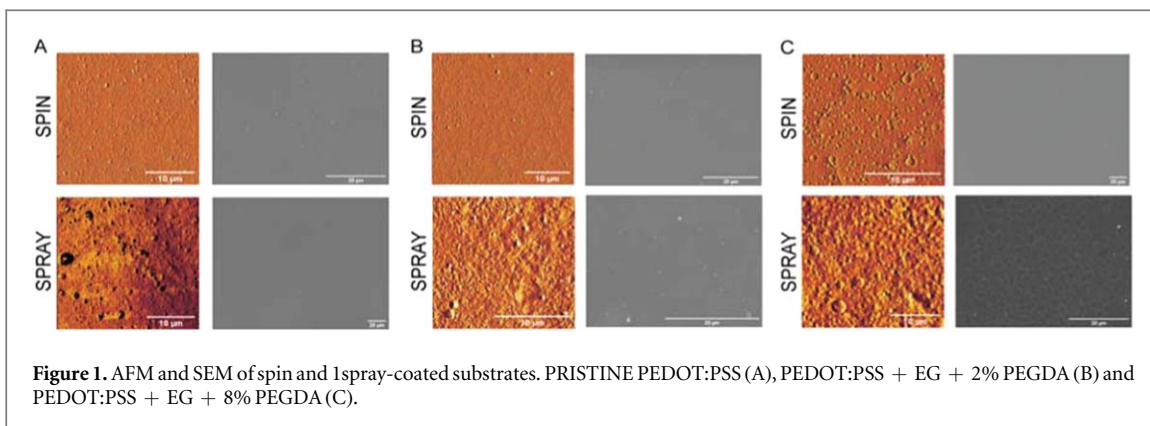
In the case of PEDOT:PSS films modified with 8% (figure 1(C)) and 17% of PEGDA (supporting information figure S1(B)), AFM highlighted grain-like areas with a variable local roughness, which substantially increases in spray-coated films. Supplementary information S2 also reports the thicknesses of the layers as measured by profilometry (RMS values were extracted from the AFM images). It is well known that PEGDA materials are 3D networks of hydrophilic polymers, characterized by the capacity to hold water within these networks. With the aim of quantifying the water uptake of our materials, the evaluation of the swelling properties of PEDOT:PSS was carried out.

The weighted amount of crosslinked blend was placed into 2 ml of PBS solution. The wet blends were weighted after 10, 20, 90 and 180 min and then dried overnight. The degree of swelling was calculated from the change in hydrogel mass when wet to swollen crosslinked blend take away of any excess liquid, as reported in:

$$\text{DOS} = \frac{(m(\text{wet}) - m(\text{dry}))}{m(\text{dry})} * 100, \quad (1)$$

where the swelling equilibrium weight is  $m(\text{wet})$  and the dry weight  $m(\text{dry})$ .

In figure 2, we observed that increasing the PEGDA concentration, the uptake of water decreases showing for PEDOT:PSS modified with 8% and 17% a high crosslinking ability [22, 26].



The effective conductivity of the films was characterized by EIS. In general, all films showed an impedance decrease with the increase of frequency as shown in figure 3, as also observed in previous

studies [35]. In particular, the lower values observed for  $|Z|$  in the high-frequency regime ( $10^4$ – $10^5$  Hz) correspond to the response of the electrolyte resistance.

**Table 1.** Value of sheet resistance, and transmittance at 550 nm of spin and spray PEDOT:PSS blends and the ratio between direct current conductivity ( $\delta_{dc}$ ) and optical conductivity ( $\delta_{op}$ ).

PEDOT:PSS blends	Rs ( $\Omega$ /sq)	T <sub>550nm</sub> (%)	$\delta_{dc}/\delta_{op}$
PRISTINE	7500	85.0	0.3
PEDOT:PSS	199	58.2	3.0
PEDOT:PSS+EG	226	86.3	10.9
	26.5	58.3	22.9
PEDOT:PSS+EG+ 2% PEGDA	175	86.8	14.6
	40	66.8	21.1
PEDOT:PSS+EG+ 8% PEGDA	154	87.3	17.4
	85	80.1	18.8
PEDOT:PSS+EG+ 17% PEGDA	168	85.2	13.4
	390	73.9	2.9

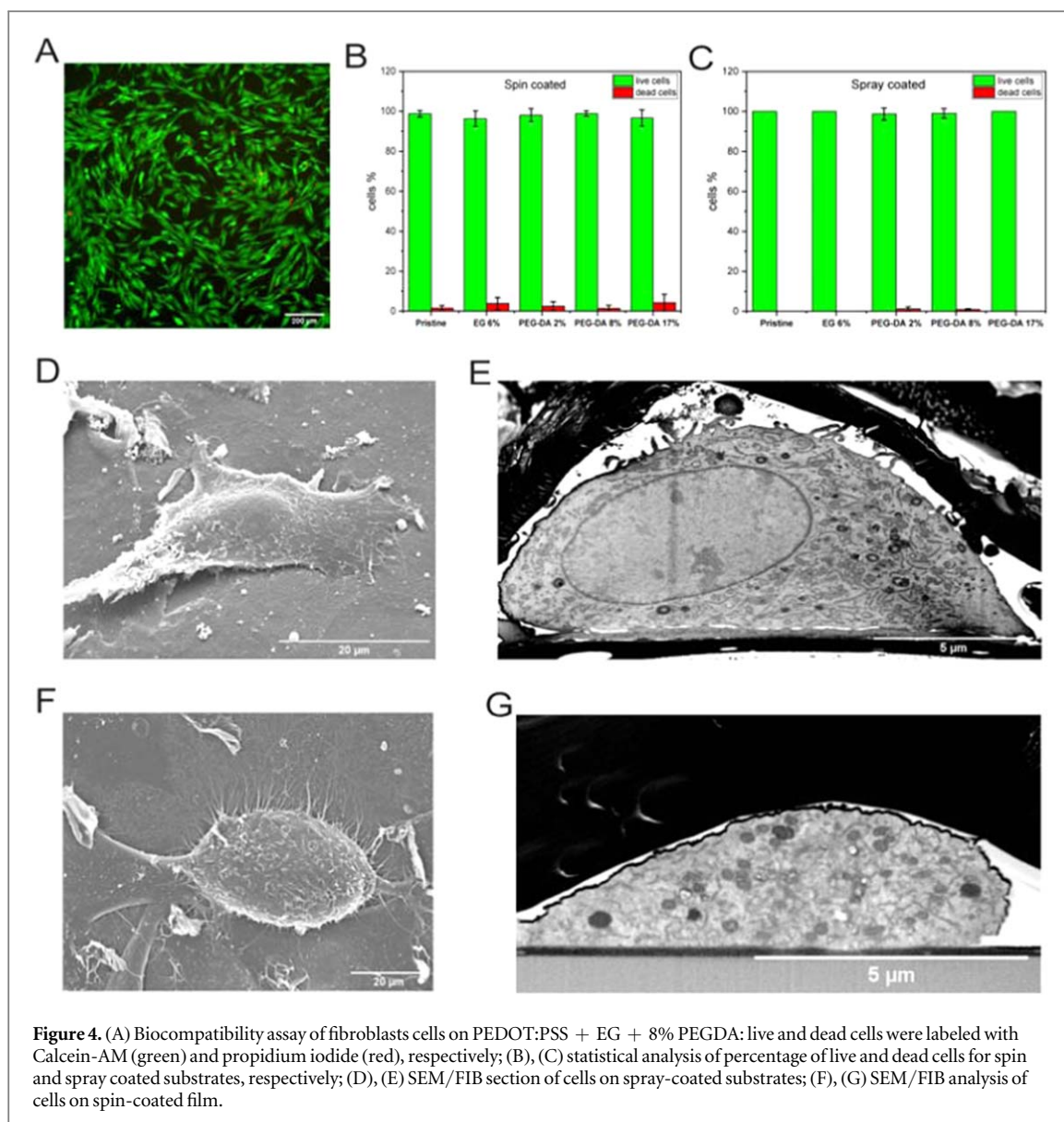
The curves showed a similar shape, with increasing impedance at low frequency, transitioning to a frequency-independent response above a characteristic frequency  $f_c$ . The impedance response above  $f_c$  was essentially the same for different types of films. Below  $f_c$  the pristine films had impedances that were higher than the corresponding modified films both for spin and spray electrodes indicating low conductivity, as expected in the case of pure PEDOT:PSS ( $850 \text{ S cm}^{-1}$ ). In particular, PEDOT:PSS shows a relevant decrease of impedance in the low-frequency regime (1–100 Hz). In the case of spin-coated (figure 3(A)) and spray-coated PEDOT:PSS modified with EG (figure 3(B)), there is a net improvement with respect to the previous case. The resulting impedance is lower if compared to the PEGDA modified blends, as expected. In addition, we reported Nyquist plots of spin and spray-coated electrodes in supplementary information S3. The behavior of PEDOT:PSS films is in accordance with previous studies [35]. Among all the resulting samples, the films containing the same concentration of PEGDA exhibited almost the same behavior for both the used techniques.

The electrodes were then characterized in terms of transmittance and sheet resistance. The electrical characteristics of transparent conductive electrodes were analyzed using Thinkam's formula [36]. The relationship between transmittance and sheet resistance is reported in terms of the ratio between direct current conductivity ( $\delta_{dc}$ ) and optical conductivity ( $\delta_{op}$ ).

In particular, higher values of  $\delta_{dc}/\delta_{op}$  indicate higher transmittance for a given sheet resistance, and

$\delta_{dc}/\delta_{op}$  must typically be  $>35$  for a known transparent film [37]. As reported in table 1, the spin-coated films are less conductive and more transmissive than spray-coated films because of their lower thickness [11]. Considering this ratio, a trade-off between transparency, conductivity, low sheet resistance ( $26.5 \text{ } \Omega$ /sq) and transmittance (58.3%), was achieved, as expected, in the case of PEDOT:PSS with 6% EG by using spray deposition (60 s results in about 180 nm thickness and  $\delta_{dc}/\delta_{op} = 22.9$ , table 1). However, despite the decrease of conductivity in the films with different amounts of PEGDA, this is still appropriate for cell stimulation [38] with optical transmittance in the range  $66.8 \div 73.9\%$  at 550 nm. The film realized with 8% of PEGDA allows obtaining the best compromise between electrical and optical performance, in particular for application in which, for instance, photo-stimulation is required. Moreover, according to the results given in figure 2, this sample is also able to exert a fairly water-repellant behavior, because of its hydrophobic nature. We reported the transmittance curves at different wavelengths and a discussion on different transmittance values in supplementary information S4.

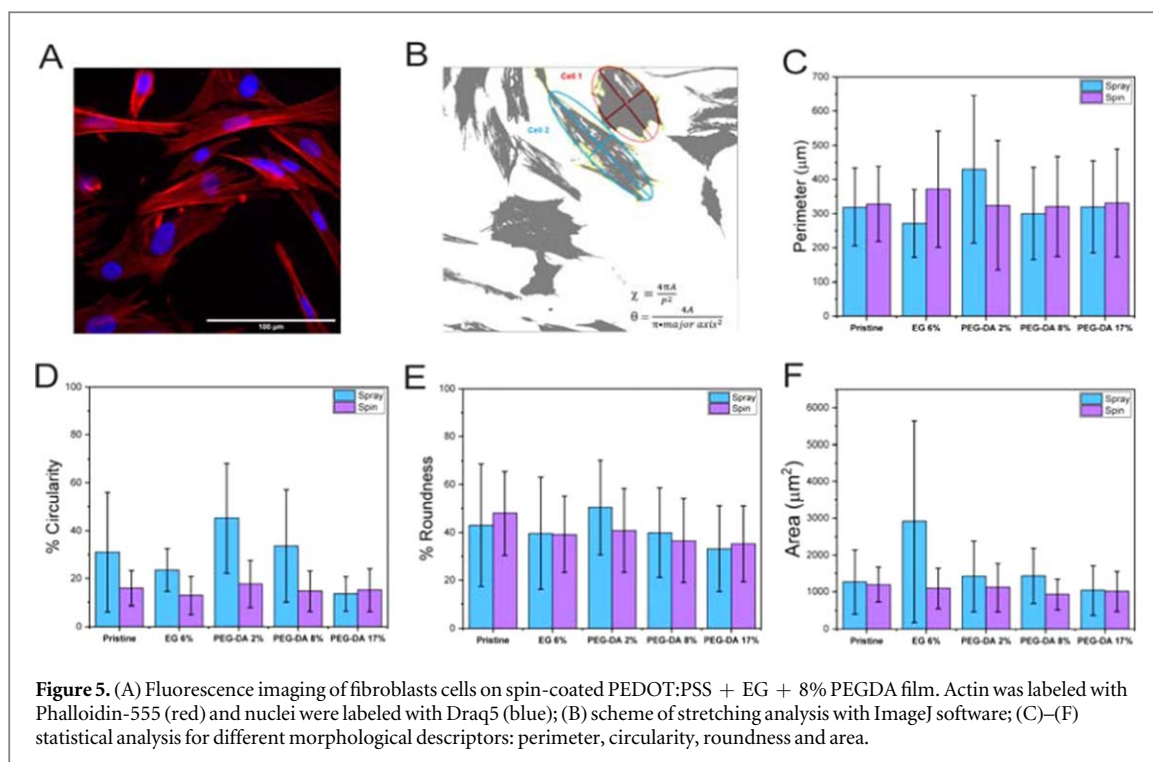
Then, the biocompatibility of the fabricated films has been assessed. In fact, we functionalized the surface of the films with poly-L-lysine in order to culture primary chicken embryo fibroblasts as described in the Materials and Methods. Two cell populations can be distinguished, labeled in green and red in figure 4(A), respectively. Figure 4(A) is an exemplary overlaid micrographs of primary cells after 1 DIV on spin-coated PEDOT:PSS + 8% PEGDA. Other exemplary



micrographs of fibroblasts on the different PEDOT:PSS blends can be found in the supplementary information S5. Effectively, cells on all PEDOT:PSS films exhibited a very high vitality ( $N = 3$ ). Cells nicely spread and adhered on the films as visible in the exemplary scanning electron micrograph of figures 4(D) and (F). Here, cells have been chemically fixed and prepared for the ultra-thin plasticization embedding procedure which allowed for the visualization of the cellular body and its protrusions in direct contact with the PEDOT:PSS-blend films underneath. The tight contact between the cellular membrane and the PEDOT:PSS films has been further investigated by performing focused ion beam sectioning as previously presented [39]. Briefly, a ROI has been located and a  $\sim 1 \mu\text{m}$  thick layer of platinum has been deposited *in situ* by subsequent electron and ion-assisted deposition. A trench out in the cell-material matrix has been performed and a fine polishing allowed to reveal the contact area between the plasma membrane and the PEDOT:PSS blend surface (figure 4(D)). By operating at 30 kV and low ion

currents (0.79–80 pA), we could achieve a smooth and defined thin section avoiding possible artefacts which might have occurred because of local heating and melting down of the polymeric PEDOT:PSS bulk. In the case of spray-coated deposition (figure 4(D)), PEDOT:PSS-blend films exhibited a rough surface, as proved by the AFM measurements, thus curtaining effects, which are typical for pseudo-3D and 3D materials when sectioned by FIB, have been further limited by the aforementioned polishing operational parameters [40]. For both spray (figures 4(D) and (E)) and spin-coated films (figures 4(F) and (G)), we found a very tight contact at the cell-material interface and a characteristic cleft which is in accordance to similar finding previously presented for HL-1 cells on planar pristine PEDOT:PSS [41].

Finally, cell spreading on PEDOT:PSS blends has been investigated by fluorescence labeling of cytoskeleton (actin filaments) and nuclei. An exemplary image of actin filaments (red signal) and nuclei (blue signal) in primary fibroblasts on spin-coated PEDOT:



PSS + EG + 8% PEGDA is shown in figure 5(A) (primary fibroblasts on the other blends are shown in supplementary information S6). Images were analyzed and cells' profiles were fit with an ellipsoidal shape in order to extract characteristic parameters such as the length of the major ( $A_{max}$ ) and minor ( $A_{min}$ ) axes, the perimeter and cell area. Moreover, two shape descriptors have been defined as shown in figure 4(B). The circularity ( $\chi$ ) gives a measure of the aspect ratio of the cell: the more this parameter is close to 0, the more elongated the cells are. The roundness ( $\theta$ ) describes the sharpness of the cells protrusions: the closer this parameter is to 0, the sharper they are. For instance, analyzing the shape descriptors for the two cells reported in figure 5(B), we find that in the case of *cell 1*, which has a more circular shape,  $\theta = 0.686$  and  $\chi = 0.174$ , while in the case of *cell 2*, which is more elongated and stretched, we have  $\theta = 0.241$  and  $\chi = 0.056$ . The perimeters of cells are comparable across all PEDOT:PSS blends and deposition techniques being in average  $\sim 300 \mu\text{m}$ . From the circularity and the roundness descriptors, we found that cells are well stretched on all films, however a rounder shape can be depicted when primary fibroblasts adhered on spray-coated PEDOT:PSS blends. This might be expected, given the surface roughness of the spray-coated films which potentially allows for more contact points of cells on to the films. Blends with PEDOT:PSS modified with 2% PEGDA resulted to be the less conductive and here, they have been identified as the culture supports where cells spread less. In contrast, PEDOT:PSS with 8% PEGDA exhibited better properties in terms of electrical conductivity and in addition, primary fibroblasts

showed the stretched conformation typical of their phenotype.

## Conclusions

In this work, we tested different PEDOT:PSS-PEGDA blends as electroactive substrates for cell cultures in order to elaborate new conductive substrates suitable for interfacing cells. In particular, we fabricated PEDOT:PSS-EG-PEGDA electrodes at increasing concentrations of PEGDA to evaluate the influence of this material on the optical, conductive and morphological properties of the films obtained via spin and spray-coating techniques. The optical and electrical analysis revealed that an optimal compromise between optical and electric properties is achieved in the case of spray PEDOT:PSS electrode modified with EG and 8% PEGDA, which also showed water retention which is compatible with bioelectronic applications. Each electrode was also tested as culture support for primary fibroblasts, proving high biocompatibility and cell spreading in all the cases. In conclusion, these results show easily processable materials which in future works can be used as patternable conductive films for integrated bioelectronic devices.

## Acknowledgments

The authors thank Fabio Formigini for the help with confocal microscopy and Manuela Ciocca for providing us some materials for electrochemical analysis.

## ORCID iDs

Giuseppina Polino  <https://orcid.org/0000-0002-6753-2103>

Aldo Di Carlo  <https://orcid.org/0000-0001-6828-2380>

Francesca Santoro  <https://orcid.org/0000-0001-7323-9504>

## References

- [1] Rivnay J, Owens R M and Malliaras G G 2014 *Chem. Mater.* **26** 679
- [2] Inal S, Rivnay J, Suiu A-O, Malliaras G G and McCulloch I 2018 *Acc. Chem. Res.* **51** 1368
- [3] Guo B and Ma P X 2018 *Biomacromolecules* **19** 1764
- [4] Balint R, Cassidy N J and Cartmell S H 2014 *Acta Biomater.* **10** 2341
- [5] Ner Y, Invernale M A, Grote J G, Stuart J A and Sotzing G A 2010 *Synth. Met.* **160** 351
- [6] Ghasemi-Mobarakeh L, Prabhakaran M P, Morshed M, Nasr-Esfahani M H and Ramakrishna S 2009 *Tissue Eng. A* **15** 3605
- [7] Zhang Y, Inal S, Hsia C-Y, Ferro M, Ferro M, Daniel S and Owens R M 2016 *Adv. Funct. Mater.* **26** 7304
- [8] Liu X, Gilmore K J, Moulton S E and Wallace G G 2009 *J. Neural Eng.* **6** 065002
- [9] Green R A, Lovell N H and Poole-Warren L A 2010 *Acta Biomater.* **6** 63
- [10] Xiao Y, Li C M, Wang S, Shi J and Ooi C P 2010 *J. Biomed. Mater. Res. A* **92** 766
- [11] Aregueta-Robles U A, Woolley A J, Poole-Warren L A, Lovell N H and Green R A 2014 *Front. Neuroeng.* **7** 15
- [12] Wen Y and Xu J 2017 *J. Polym. Sci. A* **55** 1121
- [13] Cheng W-Z, Liu J-X, Mei Y-A, Zhang P, Omi T, Takigami Y, Zhang K, Okuzaki H and Yan H 2015 *Recent Pat. Mater. Sci.* **8** 2
- [14] La Notte L, Mineo D, Polino G, Susanna G, Brunetti F, Brown T M, Di Carlo A and Reale A 2013 *Energy Technol.* **1** 757
- [15] Inal S, Hama A, Ferro M, Pitsalidis C, Oziat J, Iandolo D, Pappa A et al 2017 *Adv. Biosyst.* **1** 6
- [16] Kayser L V and Lipomi D J 2019 *Adv. Mater.* **31** 1806133
- [17] Guex A G, Puetzer J L, Armgarth A, Littmann E, Stavrinidou E, Giannelis E P, Malliaras G G and Stevens M M 2017 *Acta Biomater.* **62** 91
- [18] Zhu J 2010 *Biomaterials* **31** 4639
- [19] Nemir S, Hayenga H N and West J L 2010 *Biotechnol. Bioeng.* **105** 636
- [20] Beamish J A, Zhu J, Kottke-Marchant K and Marchant R E 2010 *J. Biomed. Mater. Res. A* **92** 441
- [21] Kim Y S, Cho K, Lee H J, Chang S, Lee H, Kim J H and Koh W-G 2016 *React. Funct. Polym.* **109** 15
- [22] Pal R K, Turner E E, Chalfant B H and Yadavalli V K 2017 *React. Funct. Polym.* **120** 66
- [23] Lu B, Yuk H, Lin S, Jian N, Qu K, Xu J and Zhao X 2019 *Nat. Commun.* **10** 1
- [24] Park H, Guo X, Temenoff J S, Tabata Y, Caplan A I, Kasper F K and Mikos A G 2009 *Biomacromolecules* **10** 541
- [25] Yuk H, Lu B and Zhao X 2019 *Chem. Soc. Rev.* **48** 1642
- [26] Bießmann L, Kreuzer L P, Widmann T, Hohn N, Moulin J-F and Müller-Buschbaum P 2018 *ACS Appl. Mater. Interfaces* **10** 9865
- [27] Xu J 2005 *Current Protocols in Molecular Biology* **70** 28.1
- [28] Belu A, Schnitker J, Bertazzo S, Neumann E, Mayer D, Offenhäusser A and Santoro F 2016 *J. Microsc.* **263** 78
- [29] Santoro F et al 2017 *ACS Nano* **11** 8320
- [30] Wang T, Qi Y, Xu J, Hu X and Chen P 2003 *Chin. Sci. Bull.* **48** 2444
- [31] Slegers S, Linzas M, Drijkoningen J, D'Haen J, Reddy N K and Deferme W 2017 *Coatings* **7** 208
- [32] Dupont S R, Voroshazi E, Heremans P and Dauskardt R H 2013 *Org. Electron.* **14** 1262
- [33] Sternling C V and Scriven L E 1959 *AIChE J.* **5** 514
- [34] Caironi M 2015 *Large Area and Flexible Electronics* (New York: Wiley)
- [35] Rivnay J et al 2015 *Sci. Adv.* **1** e1400251
- [36] Falco A, Cinà L, Scarpa G, Lugli P and Abdellah A 2014 *ACS Appl. Mater. Interfaces* **6** 10593
- [37] Alemu D, Wei H-Y, Ho K-C and Chu C-W 2012 *Energy Environ. Sci.* **5** 9662
- [38] Heo D N, Acquah N, Kim J, Lee S-J, Castro N J and Zhang L G 2018 *Tissue Eng. A* **24** 537
- [39] Li X, Matino L, Zhang W, Klausen L, McGuire A F, Lubrano C, Zhao W, Santoro F and Cui B 2019 *Nat. Protocols* **14** 1772
- [40] Santoro F, Neumann E, Panaitov G and Offenhäusser A 2014 *Microelectron. Eng.* **124** 17
- [41] Santoro F, van de Burgt Y, Keene S T, Cui B and Salleo A 2017 *ACS Appl. Mater. Interfaces* **9** 39116